

# Sputtering and Co-sputtering of Optical Coatings using a C-MAG™ Rotatable Cylindrical Cathode

A. Belkind, BOC Group Technical Center; J. Felts and M. McBride, Airco Coating Technology

**Keywords:** Optical coatings; Sputter deposition; Rotating cylindrical magnetron

## ABSTRACT

A new deposition technology for optical coatings using a C-MAG™ rotatable cylindrical magnetron cathode is reviewed. Spatial distributions of deposition rates from a dual cathode at different magnet angles were calculated and compared with experimental data. Sputtering and co-sputtering of oxides and nitrides of Al, Si, Sn, Zn, Ti, and Zr were performed. Homogeneity of the physical properties of these films was analyzed. The advantage of using a C-MAG cathode to deposit optical coatings in a large-area in-line system is discussed.

## I. INTRODUCTION

Thin film coatings on large area substrates are traditionally sputter coated with planar magnetrons<sup>1,2</sup>. During recent years, magnetron technology was successfully modified to employ unbalanced magnetrons<sup>3,4</sup> and plasma emission control.<sup>5,6</sup> Nevertheless, there are limitations on present sputtering technology including arcing, seen while depositing nonconductive oxides in the reactive mode, and low target utilization. These problems were resolved using a rotatable cylindrical magnetron.

A C-MAG rotatable cylindrical magnetron cathode was developed by Airco Coating Technology and implemented in the production of large scale thin film coatings.<sup>7-10</sup> The advantages of the rotatable cathode design are high target utilization, absence of the formation of a deep erosion groove (typical for planar magnetrons), reduced arcing during DC reactive sputtering of dielectrics, and applicability for co-sputtering in an in-line large area coater.

Co-sputtering of materials offers an important alternative to complex and sometimes impossible alloying of metallic materials for a single sputtering target.<sup>11-14</sup> Up to now, co-sputtering was accomplished with either two small, usually round cathodes<sup>11-13</sup>, or a multicomponent, tailored target.<sup>15-17</sup> In both cases, deposition of large-area homogeneous films poses serious problems. The use of C-MAG rotatable cylindrical cathodes has opened new possibilities for improved uniformity of co-sputtered films. This paper describes these developments for sputtering and co-sputtering with a C-MAG

cathode. Different aspects of sputtering and co-sputtering were reported in recent papers.<sup>18-23</sup>

## II. C-MAG CATHODE

A dual C-MAG with two targets (**Figure 1**) can rotate in any direction with variable rotation speed (a few to tens of rotations per minutes).<sup>7-9</sup> In our small coater (up to 12" × 12" substrate size), an ILS-1600 coater from Airco Coating Technology, the C-MAG cathode target diameter is 3 inches. In the larger size coaters (>12" square substrates), the target diameter is 6 inches. The targets in a dual C-MAG can each be the same or different materials.<sup>22</sup> As the cross section shows (See **Figure 1**), the target tubes rotate through the plasma which is confined by the stationary magnet assemblies placed inside of the target tubes. The magnet assemblies, in turn, can be set to any angle. Two independently operated power supplies are used with a dual C-MAG cathode when co-sputtering.

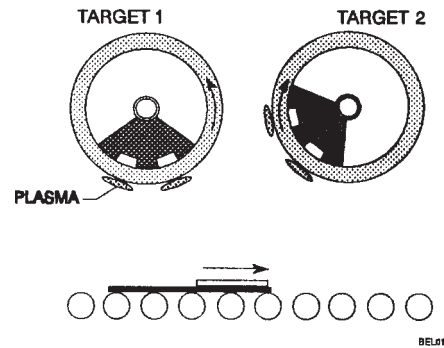


**Figure 1** - Cross-section of the sputtering system with a dual C-MAG™ rotatable cylindrical magnetron.

Deposition rate distribution along the substrate movement direction of a C-MAG cathode with vertically oriented magnet assemblies and identical targets is shown in **Figure 2**.<sup>18</sup> Turning the magnet assemblies away from each other makes the sputtered distribution more uniform, whereas turning the magnets toward each other allowed the deposition profile to be focused over a small area (**Figure 2**).

Computer modeling demonstrated that each target of the C-MAG cathode can be considered as a deposition source consisting of two sets of narrow slits located on the target surface<sup>18</sup>. Computations were done assuming that the particle emission followed a cosine distribution. Agreement between experimental data and calculations was found using two similar targets but different magnet angles (**Figure 2**).

### III. REACTIVE SPUTTERING OF OXIDES AND NITRIDES

Reactive sputtering using a C-MAG cathode reduces arcing typically observed in reactive sputtering with a planar magnetron cathode. With a planar magnetron, reactive sputtering of a nonconductive oxide is accompanied by growth of an oxide layer on the target surface outside of the race track area. The ensuing arcs are caused by charge build-up and subsequent discharge. With a C-MAG cathode, target rotation through the sputtering zone eliminates the oxide build-up except at the target edges, where sputtering does not occur. Therefore, reactive sputtering with a C-MAG cathode of  $\text{Al}_2\text{O}_3$  and  $\text{SiO}_2$  is possible.

The deposition rate of some oxides reactively sputtered with the C-MAG cathode depends on the target rotation speed.

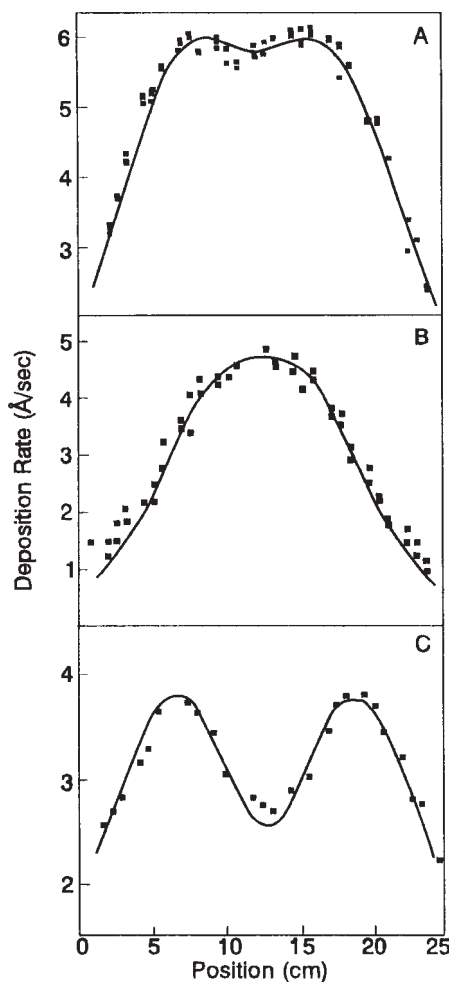


**Figure 2** - Measured (closed symbols) and calculated (open symbols) deposition rate distributions from two Al targets of a C-MAG™ 750 dual magnetron with angles of magnet assemblies of the two targets, in degrees: 0 and 0 (a), 20 and -20 (b), -30 and 30 (c), respectively. Deposition conditions: 2 kW power on each target; 2.7 mTorr total pressure; 20 sccm and 25 sccm of Ar and  $\text{O}_2$  flow rates, respectively.

For example, the deposition rate of  $\text{TiO}_2$  increased with decreasing target rotation speed.<sup>23</sup> Slower target rotation also broadened the hysteresis curve. This effect was shown to be consistent with a model where the tube surface was oxidized outside of the active sputtering region. The oxidized surface was subsequently brought into the sputtering zone by the rotation of the target and sputtered away.

Some oxides;  $\text{SiO}_2$ ,  $\text{Al}_2\text{O}_3$ ,  $\text{ZnO}$ ,  $\text{ZrO}_2$  and  $\text{TiO}_2$ , and nitrides,  $\text{Si}_3\text{N}_4$ ,  $\text{ZrN}$ , and  $\text{TiN}$  were sputtered with the C-MAG cathode. All of these compounds were deposited in several machines ranging from the Airco Coating Technology ILS-1600 (12"×12" substrates) to an automotive coater capable of coating curved substrates in widths over 1 meter. Targets used in the work were: self-supported tubes of zirconium, aluminum, and titanium, cast tubes of zinc and tin, and plasma sprayed silicon. The plasma sprayed and cast targets were supported by a stainless steel backing tube<sup>22</sup>. Some typical deposition conditions of these oxides and nitrides in an ILS-1600 in-line system are listed in Table 1. DDR is the dynamic deposition rate in  $\text{Å}\cdot\text{mm}^2/\text{Joule}$ , determined as:<sup>2</sup>

$$\text{DDR} = \frac{(d \times L \times v)}{(P \times n)}$$

where d is the film thickness in angstroms, L is the target race-track length in mm, v is the substrate (conveyor) speed in mm/sec, P is the power applied in watts, and n is the number of passes.

**Table 1**

Material	Power (kW)	Ar (sccm)	$\text{O}_2/\text{N}_2$ (sccm)	Press. Pa	DDR	Refr. index <sup>b</sup>
$\text{SiO}_2$	4.0	12	31	2.1	510	1.46
$\text{TiO}_2$	6.0	20	30	1.6	85	2.51
$\text{Al}_2\text{O}_3$	3.0	35	15	2.8	200	1.63
$\text{Si}_3\text{N}_4$	4.0	60	12	2.1	2600	2.0
$\text{TiN}^c$	9.0	30	39	1.3	1400	

a -  $\text{O}_2$  or  $\text{N}_2$ , b - at 632.8 nm, and c - 85  $\mu\Omega\cdot\text{cm}$  resistivity

Rutherford back-scattering and FT-IR analyses of silicon oxide and silicon nitride showed that their respective compositions were close to stoichiometric  $\text{SiO}_2$  and  $\text{Si}_3\text{N}_4$  (within the limit of measurement errors).

The  $\text{SiO}_2$ ,  $\text{Si}_3\text{N}_4$ , and  $\text{TiO}_2$  films deposited using the C-MAG cathode had higher refractive indices and better abrasion resistance than films made using a planar magnetron<sup>8</sup>. The C-MAG cathode employs an unbalanced magnetic field, enhancing substrate bombardment during deposition. Substrate bombardment increased film density resulting in the observed higher refractive index and better mechanical performance.

## IV. REACTIVE CO-SPUTTERING OF OXIDES AND NITRIDES

### 4.1 Inhomogeneity of a Film Deposited on a Dynamic Substrate

The composition of a co-sputtered film should be homogeneous in depth. The composition in depth distribution of a film deposited on a moving substrate is determined by comparing the sputtered flux at all points along the substrate path. For sputtering in an in-line system using a C-MAG cathode with magnet angles of  $0^\circ$  and two targets of different materials, as the substrate enters the deposition chamber, the obliquely sputtered flux from target A is deposited first (Figure 3). Moving the substrate further, the over-lapping fluxes of material A and B form the second and principal layer of interest. As the substrate exits from the sputtering zone, an obliquely sputtered flux from target B is deposited resulting in a three-layer coating. The first layer is from the first target material with a graded interface between it and the second layer. The second layer is the co-sputtered material of interest. The third layer is formed by a graded interface with an overlying film of the second target material. The film stack produced will look like Figure 3. By tilting the magnets, the first and third layer thicknesses were minimized resulting in a single co-sputtered material layer (the middle layer). The magnet angle must be optimized to minimize the first and third layer effects while maintaining the highest deposition rate. Turning the magnets to face each other enhances target cross-contamination. Target cross-contamination while co-sputtering using planar magnetrons was previously considered a detri-

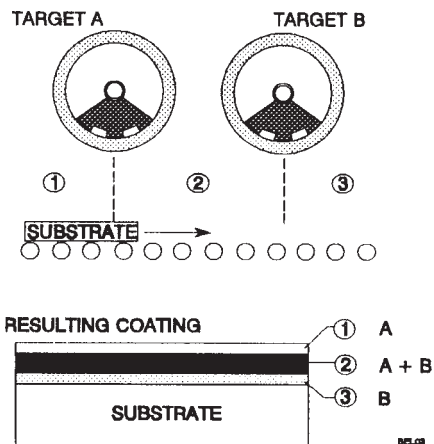


Figure 3 - Three layer model for co-sputtering on a dynamic substrate using a C-MAG™ cathode with targets from material A and B.

mental factor<sup>12</sup>. Co-sputtering with a C-MAG rotatable cylindrical cathode, however, requires target cross-contamination to deposit homogeneous films.

### 4.2 Magnet Angle Effect

Composition distribution of films deposited along the center axis of the substrate was different for differing magnet angles (Figure 4a). When magnet angles were greater than  $30^\circ$  (towards each other), the distribution became substantially homogeneous (Figure 4a). Changing the magnet angles by  $15^\circ$  gave composition distributions with about  $\pm 5\%$  or better of the individual material in the mixed matrix. For example, magnet angles of  $30^\circ$  (Zn target) and  $45^\circ$  (Sn target) during co-sputtering ZnO and SnO<sub>2</sub> gave  $\pm 1\%$  for the calculated ZnO/SnO<sub>2</sub> compositions (Figure 5). For TiO<sub>2</sub> and ZrO<sub>2</sub>  $\pm 4\%$  was found using magnet angles of  $60^\circ$  (Ti) and  $30^\circ$  (Zr) (Figure 5). Varying the power applied to the two targets altered the homogeneity slightly (Figure 5).

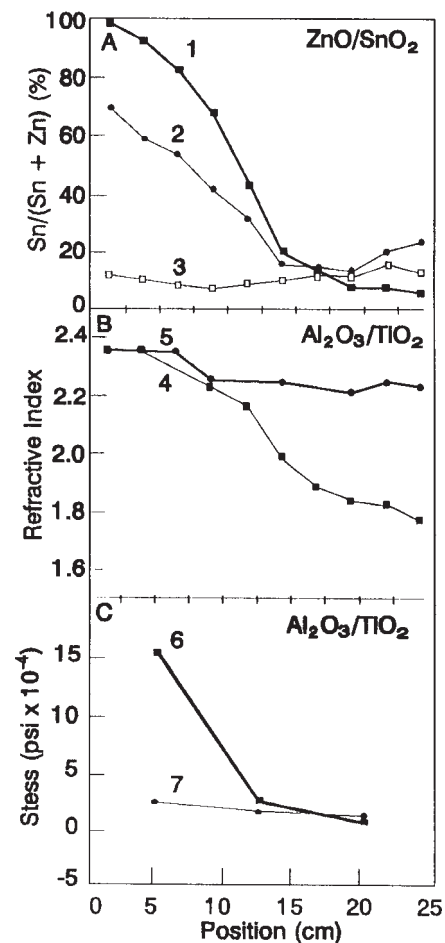
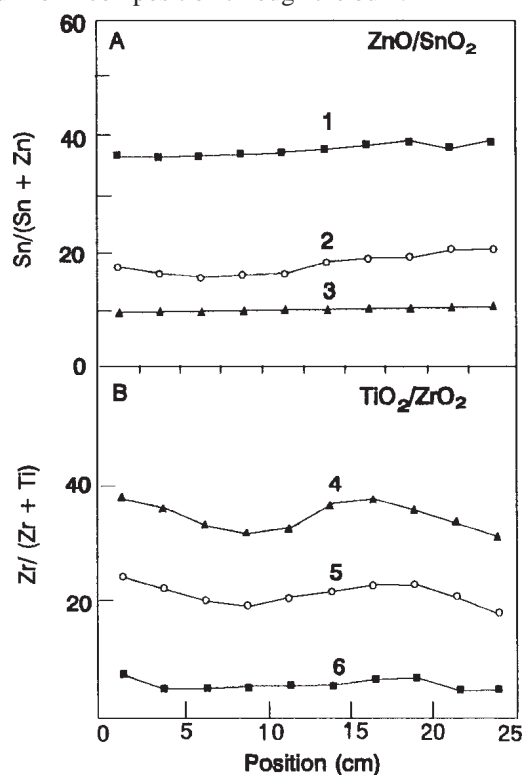


Figure 4 - Distribution of composition (a), refractive index (b), and stress (c) of co-sputtered films deposited along the central line with facing each other angles of magnet assemblies, in degrees: 0,0 (1), 30,30 (2), 30, 45 (3), 0/0 (4), 25, 25 (5), 0/0 (6), and 30/30 (7).

To evaluate the importance of the geometry on cross-contamination, the composition distribution of co-sputtered films was compared with calculated distributions assuming no target cross-contamination.<sup>18</sup> The calculated distributions were determined by the ratio of deposition rates from each individual target. The comparison of these distributions showed that with 0° magnet angles, the experimental and calculated distributions matched (**Figure 6a**), so cross-contamination was not important. When the magnet angles were  $\geq 30^\circ$ , the experimental data was significantly different than calculated (**Figure 6b**); therefore, target cross-contamination dominated.

In the presence of target cross-contamination, target rotation improved the homogeneity of distribution by making the composition of the target surface more uniform.

Composition distribution through the bulk of the films deposited on dynamic substrates using optimal magnet angles are shown in **Figure 7**. As expected, the optimal magnet angle gave uniform composition through the bulk.



**Figure 5** - Distribution of composition of co-sputtered films of ZnO and SnO<sub>2</sub> (a), and TiO<sub>2</sub> and ZrO<sub>2</sub> (b) deposited along the central line using different powers. Power applied to the Sn and Zn targets, in kW: 0.25 and 0.6 (1), 0.5 and 0.6 (2), 0.5 and 0.3 (3). Power applied to the Ti and Zr targets, in kW: 4 and 1 (4), 4 and 1.5 (5), 4 and 2 (6). Angles of magnet assemblies (facing each other) of the Sn, Zn, Ti and Zr targets, in degrees: 30, 45, 60 and 30, respectively.

### 4.3 Physical Properties of Co-Sputtered Films

Co-sputtering at magnet angles that provide homogeneous material distributions also results in homogeneous distributions of physical properties. As an example, distribution of refractive index and stress of some co-sputtered films are shown in Figure 4b and 4c. Magnet angle optimization also allows one to develop coatings with desirable properties. Most of the co-sputtered films were either amorphous or showed much less crystallinity than the films of the individual materials. For example, traces of the rutile phase were found in the x-ray diffraction spectra of TiO<sub>2</sub> films. Mixed TiO<sub>2</sub>/ZrO<sub>2</sub> films were amorphous. Film amorphization has been obtained on many mixed materials.<sup>21,24-26</sup> Stress of the most analyzed co-sputtered films was less than the stress of films of the individual components (Figure 4c). For example, the stress of AlSixNy was 60 kPsi, while AlN and Si<sub>3</sub>N<sub>4</sub> were expected to be 150 kPsi. In the case of AlSiOx the stress was 10 kPsi, while Al<sub>2</sub>O<sub>3</sub> is 40 kPsi and SiO<sub>2</sub> was 18 kPsi. Stress reduction through mixing materials was shown previously<sup>21,25,27,28</sup> and was attributed to changes in grain size and intergrain forces.<sup>28</sup>

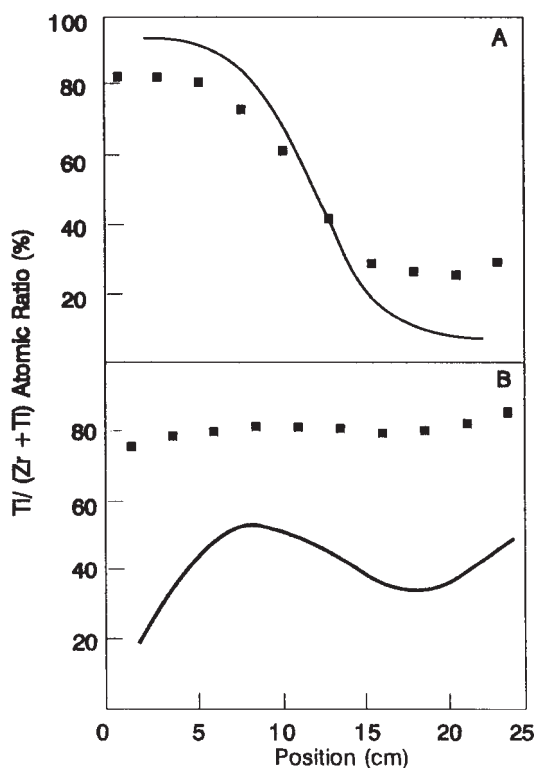


**Figure 6** - Measured (squares) and calculated distribution of composition of co-sputtered films deposited along the central line from a C-MAG™ 750 dual magnetron with angles of magnet assemblies of the Ti and Zr targets, in degrees: 0 and 0 (a), and 60 and 30, respectively. Deposition conditions: 4.0 kW and 1.5 kW on Ti and Zr targets, respectively; 3.7 mTorr total pressure; 35 sccm and 40 sccm of Ar and O<sub>2</sub> flow rates, respectively.

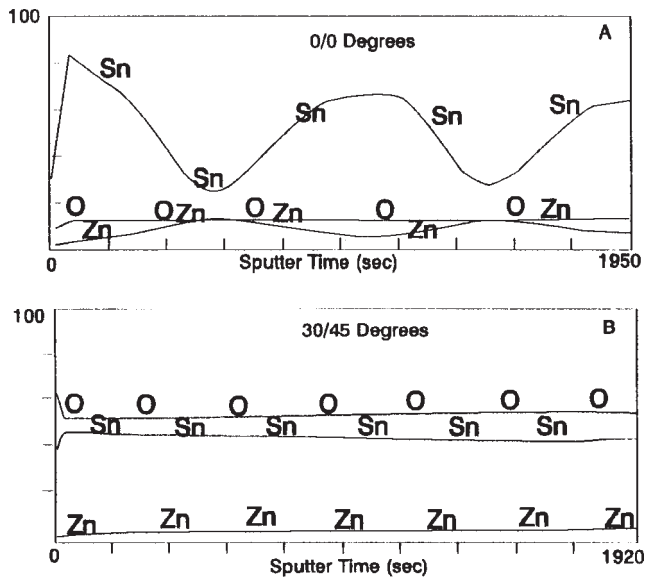


Figure 7 - Composition through the bulk of co-sputtered ZnO and SnO<sub>2</sub> films deposited using angles of magnet assemblies of the Zn and Sn targets, in degrees: 0 and 0 (a), and 30 and 45 (b), respectively.

## V. CONCLUSION

A C-MAG cathode can be successfully used to deposit various optical coatings: Al<sub>2</sub>O<sub>3</sub>, SiO<sub>2</sub>, TiO<sub>2</sub>, ZnO, SnO<sub>2</sub>. Deposition of non-conductive coatings as Al<sub>2</sub>O<sub>3</sub> and SiO<sub>2</sub> can be accomplished with minimal arcing.

In the first approximation, the spatial distribution of deposition rate from a C-MAG cathode can be computed considering it to consist of two sets of narrow planar segments located at the cylindrical target surface emitting particles in a cosine distribution.

Similarity in total pressure vs. oxygen flow rate hysteresis curves for sputtering and co-sputtering showed that these two processes were alike.

Co-sputtering using a C-MAG cathode allowed mixed materials to be deposited with a homogeneous distribution. Film homogeneity was achieved by inclining the magnets to angles around 30° and by rotating the targets. Substantial target cross-contamination was obtained at these magnet angles. Films of mixed oxides and nitrides were less crystalline and had lower stress than films of the individual materials.

## REFERENCES

1. A.D. Grubb, T.S. Mosakowski, W.G. Overacker, Proc. SPIE, 325 (1982) 74.
2. D. Griffin, Proc. SPIE, 823 (1987) 7.
3. B. Window and N. Savvides, J. Vac. Sci. Technol. A4 (1986) 196.
4. N. Savvides and B. Window, J. Vac. Sci. Technol. A4 (1986) 504.
5. S. Schiller, U. Heisig, K. Steinfelder, J. Strumpf, R. Voigt, R. Fendler, and Teschner, Thin Solid Films, 96 (1982) 235.
6. K. Enjouji, K. Murata, and S. Nishikawa, Thin Solid Films, 108 (1983) 1.
7. J.J. Hofmann, Proc. 32nd Annual Techn. Conf., Society of Vacuum Coaters, 1989, p. 297.
8. C. Boehmler, Proc., Third International Conference on Vacuum Web Coating, 1989, p. 222.
9. B.P. Barney, Proc. 33rd Annual Tech. Conf., Society of Vacuum Coaters, 1990, p. 43.
10. M.W. McBride, Proc. 33rd Annual Tech. Conf., Society of Vacuum Coaters, 1990, p. 250.
11. W.R. Sinclair and F.G. Peters, Rev. Sci. Instr., 33 (1962) 744.
12. J.J. Hanak, Le Vide, 175 (1975) 11.
13. C. Misiano and E. Simonetti, Vacuum, 27 (1977) 403.
14. B.J. Pond, J.I. DeBar, C. Carnigia, and T. Raj, in Optical Interference Coatings, Technical Digest Series, Optical Society of America, Washington, D.C., 6 (1988) 2085.
15. C.M. Gilmore, C. Quinn, S.B. Quadri, C.R. Gossett, and E.F. Skelton, J. Vac. Sci. Technol. A5 (1987) 2085.
16. K. Nomura, N. Ogawa, and A. Abe, J. Electrochem. Soc., 134 (1987) 922.
17. E. Broese and W. Heerdegen, Postdamer Forsch. Paedagog. Hochsch. "Karl Liebknecht" Potsdam, Naturwiss. Reihe, 53 (1987) 7.
18. A. Belkind, W. Gerristead, and Z. Orban, to be published.
19. A. Belkind, E. Ezell, W. Gerristead, Z. Orban, P. Rafalko, D. Dow, J. Felts, and R. Laird, J. Vac. Sci. Technol., to be published.
20. J. Wolfe, to be published.
21. A. Belkind, W. Gerristead, Z. Orban, D. Dow, J. Felts, and R. Laird, to be published.
22. J. Hillendahl, to be published.
23. P. Sieck, A. Belkind, and Z. Orban, to be published.
24. A. Feldman, E.N. Farabaugh, W.K. Haller, D.M. Sanders, and R.A. Stempniak, J. Vac. Sci. Technol. A4 (1986) 2969.
25. H. Sankur and W.J. Gunning, J. Appl. Phys. 66 (1989) 4747.
26. M.A. Russak, C.V. Jahnes, and E.P. Katz, J. Vac. Sci. Technol. A4 (1989) 1248.
27. C. Misiano, M. Varasi, C. Mancini, and P. Sartori, Le Vide, Couches Minces, 212 Suppl. (1982) 149.
28. H. Sankur, W.J. Gunning, and J.F. DeNatale, Appl. Opt. 27 (1988) 1564.